Astro Ltd.

**LETTER**

# A self-bound matter-wave boson–fermion quantum ball

View the article online for updates and enhancements.

## Related content

- Statics and dynamics of a self-bound dipolar matter-wave droplet
  S K Adhikari

- Stable and mobile excited two-dimensional dipolar Bose–Einstein condensate solitons
  S K Adhikari

- Stable matter-wave solitons in the vortex core of a uniform condensate
  S K Adhikari

## Recent citations

- Self-trapped quantum balls in binary Bose–Einstein condensates
  Sandeep Gautam and S K Adhikari

- A fermionic impurity in a dipolar quantum droplet
  Matthias Wenzel *et al*

**IOP ebooks™**

Bringing you innovative digital publishing with leading voices to create your essential collection of books in STEM research.

Start exploring the collection - download the first chapter of every title for free.

# Letter

# A self-bound matter-wave boson–fermion quantum ball

## S K Adhikari

Instituto de Física Teórica, UNESP–Universidade Estadual Paulista, 01.140-070 São Paulo, São Paulo, Brazil

E-mail: adhikari44@yahoo.com

## Abstract

We demonstrate the possibility of creating a self-bound stable three-dimensional matter-wave spherical boson–fermion quantum ball in the presence of an attractive boson–fermion interaction and a small repulsive three-boson interaction. The two-boson interaction could be attractive or repulsive whereas the fermions are taken to be in a fully-paired super-fluid state in the Bardeen–Cooper–Schreifer (quasi-noninteracting weak-coupling) limit. We also include the Lee–Huang–Yang (LHY) correction to a repulsive bosonic interaction term. The repulsive three-boson interaction and the LHY correction can stop a global collapse while acting jointly or separately. The present study is based on a mean-field model, where the bosons are subject to a Gross–Pitaevskii (GP) Lagrangian functional and the fully-paired fermions are described by a Galilean-invariant density functional Lagrangian. The boson–fermion interaction is taken to be the mean-field Hartree interaction, quite similar to the interaction term in the GP equation. The study is illustrated by a variational and a numerical solution of the mean-field model for the boson–fermion $^7$Li–$^6$Li system.

Keywords: Bose–Einstein condensate, superfluid fermion, soliton

(Some figures may appear in colour only in the online journal)

## 1. Introduction

A self-bound matter-wave bright soliton can travel with a constant velocity in one-dimension (1D) [1], while maintaining its shape, due to a balance between defocusing forces and nonlinear attraction. Solitons have been observed in diverse systems obeying classical and quantum dynamics, such as, in water wave, nonlinear optics [2] and Bose–Einstein condensate (BEC) [3] among others. The 1D soliton could be analytic with energy and momentum conservation necessary to maintain its shape during propagation. However, such a soliton cannot be realized in three dimensions in the mean-field weak-coupling Gross–Pitaevskii (GP) limit due to a collapse instability for attractive interaction [1, 2].

On the theoretical front Petrov [4] demonstrated the possibility of a three-dimensional (3D) binary BEC droplet in the presence of an inter-species attraction and an intra-species repulsion with a Lee–Huang–Yang (LHY) correction [5]. The possibility of forming a binary 1D BEC soliton with intra-species repulsion and inter-species attraction was suggested before [6]. In the presence of a repulsive three-body interaction the statics and dynamics of a BEC quantum ball were studied in details recently [7] employing the numerical and variational solutions of a mean-field model. A droplet can also be realized in a spin–orbit- [8] or Rabi-coupled [9] multi-component spinor BEC. On the experimental front, a BEC droplet has been observed [10] in a dipolar dysprosium and erbium BEC with a repulsive short-range contact interaction. Later, the formation of the dipolar droplet has been explained [11] by a LHY correction to the short-range contact interaction. More recently, a binary BEC droplet has been observed in the presence of a repulsive intra-species interaction and an

attractive inter-species interaction [12, 13] and its formation was explained by including a LHY-type correction term to the intra-species repulsion.

We demonstrate that it is possible to bind a large number of spin-1/2 fermions in a self-bound 3D boson–fermion superfluid quantum ball at zero temperature in the presence of an attractive boson–fermion interaction and a repulsive three-boson interaction together with the LHY correction for a repulsive boson–boson interaction. We prefer the name quantum ball over droplet for the localized boson–fermion state after establishing the robustness of such a bosonic state to maintain the spherical ball-like structure after collision [7], in contrast to easily deformable liquid droplets. Due to Pauli repulsion it is difficult to bind the fermions: the bosons with an attractive inter-species interaction act like a glue to bind the fermions. The possibility of binding fermions in a 1D boson–fermion mixture without a trap in the presence of inter-species attraction was suggested theoretically [14], and later realized experimentally [15]. In this study, we take the fermions to be fully paired in a quasi-noninteracting weak-coupling super-fluid Bardeen–Cooper–Schrieffer (BCS) state, although this condition is not required for binding; all fermions in a spin-polarized state can also be bound in a boson–fermion quantum ball. The repulsive three-boson interaction and its LHY correction lead to terms with a higher order nonlinearity in the dynamical 'mean-field' boson–fermion equation, compared to the nonlinearity resulting from the boson–boson interaction, and create a strong repulsive core at the origin and hence stop a global collapse of the boson–fermion mixture and stabilize the quantum ball.

We consider a numerical and a variational solution of a mean-field model for the formation of the boson–fermion quantum ball. The Lagrangian functional of the bosons is taken as in the GP Lagrangian functional including a three-boson interaction term and a LHY correction for a repulsive boson–boson interaction and that of the fermions is taken as a Galilean invariant density functional Lagrangian [16]. The boson–fermion interaction is taken as the interaction term in the GP Lagrangian functional [17]. The Euler–Lagrange equations for the Lagrangian functional lead to a coupled set of equations employed in this study. We illustrate the formation of a boson–fermion quantum ball in the $^7$Li–$^6$Li mixture using realistic values of different parameters.

In section 2 the mean-field model for the boson–fermion mixture is developed. A time-dependent, analytic, Euler–Lagrange Gaussian variational approximation of the model is also presented. The results of numerical calculation are shown in section 3. Finally, in section 4 we present a brief summary of our findings.

## 2. Analytic model for a boson–fermion quantum ball

We consider a binary boson–fermion super-fluid mixture at zero temperature interacting via inter- and intra-species interactions with the mass and number of the two species $i = 1, 2$, denoted by $m_i, N_i$, respectively. The first species ($^7$Li) is taken

to be bosons while the second species ($^6$Li) fermions. The spin-half fermions are assumed to be fully paired with an equal number of spin-up and -down atoms. We start by writing the Lagrangian density of the system

$$\mathcal{L} = \Big[ \sum_i i\hbar \frac{N_i}{2} (\phi_i \dot{\phi}_i^* - \phi_i^* \dot{\phi}_i) + \frac{N_1 \hbar^2}{2m_1} |\nabla \phi_1|^2$$
$$+ \frac{N_2 \hbar^2}{8m_2} |\nabla \phi_2|^2 + \frac{1}{3} \frac{\hbar N_1^3 K_3}{2} |\phi_1|^6 + \frac{1}{2} \frac{4\pi \hbar^2 a_1}{m_1} N_1^2 |\phi_1|^4$$
$$+ \frac{2}{5} \frac{2\hbar^2}{m_1} \pi \alpha a_1^{5/2} N_1^{5/2} |\phi_1|^5 + \frac{1}{2} 4\pi a_{12} N_1 N_2 \frac{\hbar^2}{m_R} |\phi_1|^2 |\phi_2|^2$$
$$+ \frac{3}{5} \frac{\hbar^2}{2m_2} N_2 (3\pi^2 N_2)^{2/3} |\phi_2|^{10/3} \Big], \quad i = \sqrt{-1}, \tag{1}$$

where $a_1$ is the scattering length of bosons (component 1), $a_{12}$ is the boson–fermion scattering length, $m_R = m_1 m_2 / (m_1 + m_2)$ is the boson–fermion reduced mass and the overhead dot denotes time derivative. In (1) the first term on the right is the usual time-dependent term [16, 18], the second and the third terms represent the kinetic energies of bosons and fermions, respectively [16], the term containing $K_3$ is the three-boson interaction term. The prefactor $N_2 \hbar^2 / 8m_2$ in the fermion kinetic energy guarantees Galilean invariance of the Lagrangian [16]. The next term proportional to $a_1$ is the interaction energy of bosons and that proportional to $a_{12}$ is the boson–fermion interaction energy. The term containing $\alpha \equiv 64/(3\sqrt{\pi})$ represents the beyond-mean-field LHY correction to the repulsive bosonic intra-atomic interaction ($a_1 > 0$). The fermions are assumed to be quasi-noninteracting in a completely full Fermi sea and contributes the term proportional to $|\phi_2|^{10/3}$ in (1), which is just the static kinetic energy of all the fermions [16]. Both the three-body and the LHY terms have higher-order nonlinearity compared to the two-body interaction term, viz. the term containing $a_1$ in (1). These terms with a positive real part of $K_3$ guarantee a large positive energy near the origin $\mathbf{r} = 0$ and stop the collapse of the system.

It is convenient to write a dimensionless form of expression (1) as

$$\mathcal{L} = \Big[ \sum_i i \frac{N_i}{2} (\phi_i \dot{\phi}_i^* - \phi_i^* \dot{\phi}_i) + \frac{N_1}{2} |\nabla \phi_1|^2 + \frac{m_1}{8m_2} N_2 |\nabla \phi_2|^2$$
$$+ 2\pi a_1 N_1^2 |\phi_1|^4 + \frac{4}{5} \pi \alpha a_1^{5/2} N_1^{5/2} |\phi_1|^5 + \frac{N_1^3 K_3}{6} |\phi_1|^6$$
$$+ \frac{3m_1}{10m_2} N_2 (3\pi^2 N_2)^{2/3} |\phi_2|^{10/3}$$
$$+ 2\pi a_{12} N_1 N_2 \frac{m_1}{m_R} |\phi_1|^2 |\phi_2|^2 \Big], \quad i = \sqrt{-1}, \tag{2}$$

where length is expressed in units of a fixed length $l$, density $|\phi_i|^2$ in units of $l^{-3}$, time in units of $t_0 = m_1 l^2 / \hbar$, energy in units of $\hbar^2 / m_1 l^2$ and $K_3$ in units of $\hbar l^4 / m_1$. The wave functions are normalized as $\int |\phi_i|^2 d\mathbf{r} = 1$.

With Lagrangian density (2) the dynamics for the binary boson–fermion mixture is governed by the Euler–Lagrange equations

$$\frac{d}{dt}\frac{\partial \mathcal{L}}{\partial \dot{\psi}_i^*} = \frac{\partial \mathcal{L}}{\partial \psi_i^*}. \quad (3)$$

In explicit notation (3) become [18]

$$i\frac{\partial \phi_1(\mathbf{r},t)}{\partial t} = \Big[ -\frac{\nabla^2}{2} + 4\pi a_1 N_1 |\phi_1|^2 + \frac{K_3 N_1^2}{2}|\phi_1|^4$$
$$+ 2\pi \alpha a_1^{5/2} N_1^{3/2}|\phi_1|^3 + \frac{2\pi m_1 a_{12} N_2}{m_R}|\phi_2|^2 \Big] \phi_1(\mathbf{r},t), \quad (4)$$

$$i\frac{\partial \phi_2(\mathbf{r},t)}{\partial t} = \Big[ -\frac{m_1\nabla^2}{8m_2} + \frac{m_1}{2m_2}(3\pi^2 N_2)^{2/3}|\phi_2|^{4/3}$$
$$+ \frac{2\pi m_1 a_{12} N_1}{m_R}|\phi_1|^2 \Big] \phi_2(\mathbf{r},t). \quad (5)$$

Convenient analytic variational approximation to (4) and (5) can be obtained with the following Gaussian ansatz for the wave functions [18, 19]

$$\phi_i(\mathbf{r},t) = \frac{\pi^{-3/4}}{w_i(t)\sqrt{w_i(t)}} \exp\Big[ -\frac{r^2}{2w_i^2(t)} + i\beta_i(t)r^2 \Big] \quad (6)$$

where $w_i$ are the widths and $\beta_i$ are additional variational parameters, called chirps. The effective Lagrangian for the binary system $L = \int d\mathbf{r}\mathcal{L}$ is

$$L = \sum_{i=1}^{2} \frac{N_i}{2} 3w_i^2 \dot{\beta}_i + \frac{N_1}{2}\Big[ \frac{3}{2w_1^2} + 6w_1^2\beta_1^2 \Big]$$
$$+ \frac{N_2 m_1}{8m_2}\Big[ \frac{3}{2w_2^2} + 6w_2^2\beta_2^2 \Big] + \frac{N_1^2 a_1}{\sqrt{2\pi}w_1^3}$$
$$+ \frac{8\sqrt{2}}{25\sqrt{5}}\frac{\alpha a_1^{5/2}N_1^{5/2}}{\pi^{5/4}w_1^{9/2}} + \frac{N_1^3 K_3}{18\sqrt{3}\pi^3 w_1^6}$$
$$+ \frac{9\sqrt{3}m_1(3\pi^2 N_2)^{2/3}N_2}{50\sqrt{5}m_2\pi w_2^2} + \frac{2a_{12}m_1 N_1 N_2}{\sqrt{\pi}m_R(w_1^2+w_2^2)^{3/2}}. \quad (7)$$

The repulsive three-boson $K_3$-dependent term with a $1/w_1^6$ divergence and the LHY two-boson $\alpha$-dependent term with a $1/w_1^{9/2}$ divergence at the origin ($w_1 = w_2 = 0$) create a repulsive core in the Lagrangian $L(w_1, w_2)$ which stops the global collapse.

The four Euler–Lagrange variational equations of the effective Lagrangian $L$ for the four variational parameters $\alpha \equiv w_1, w_2, \beta_1, \beta_2$

$$\frac{d}{dt}\frac{\partial}{\partial \dot{\alpha}} = \frac{\partial L}{\partial \alpha}, \quad (8)$$

can be simplified to yield the following coupled ordinary differential equations for the widths, $w_i$ in usual fashion [19]

$$\ddot{w}_1 = \frac{1}{w_1^3} + \frac{2N_1 a_1}{\sqrt{2\pi}w_1^4} + \frac{2N_1^2 K_3}{9\sqrt{3}\pi^3 w_1^7} + \frac{4a_{12}m_1 N_2 w_1}{\sqrt{\pi}m_R(w_1^2+w_2^2)^{5/2}}$$
$$+ \frac{24\sqrt{2}}{25\sqrt{5}}\frac{\alpha a_1^{5/2}N_1^{3/2}}{\pi^{5/4}w_1^{11/2}}, \quad (9)$$

$$\ddot{w}_2 = \frac{m_1}{4m_2 w_2^3} + \frac{6\sqrt{3}m_1(3\pi^2 N_2)^{2/3}}{25\sqrt{5}m_2\pi w_2^3} + \frac{4a_{12}m_1 N_1 w_2}{\sqrt{\pi}m_R(w_1^2+w_2^2)^{5/2}}. \quad (10)$$

The solution of the time-dependent equations (9)–(10) gives the dynamics of the variational approximation. For static properties of the boson–fermion quantum ball, the time derivatives in these equations should be set equal to zero.

The energy of the system is given by

$$E = \frac{3N_1}{4w_1^2} + \frac{3N_2 m_1}{16m_2 w_2^2} + \frac{N_1^2 a_1}{\sqrt{2\pi}w_1^3} + \frac{N_1^3 K_3}{18\sqrt{3}\pi^3 w_1^6}$$
$$+ \frac{8\sqrt{2}}{25\sqrt{5}}\frac{\alpha a_1^{5/2}N_1^{5/2}}{\pi^{5/4}w_1^{9/2}} + \frac{9\sqrt{3}m_1(3\pi^2 N_2)^{2/3}N_2}{50\sqrt{5}m_2\pi w_2^2}$$
$$+ \frac{2a_{12}m_1 N_1 N_2}{\sqrt{\pi}m_R(w_1^2+w_2^2)^{3/2}}. \quad (11)$$

The widths of the stationary state can be obtained from the solution of equations (9) and (10) setting the time derivatives of the widths equal to zero. This procedure is equivalent to a minimization of the energy (11), provided the stationary state corresponds to a energy minimum.

## 3. Numerical results

The 3D binary mean-field equations (4) and (5) do not have analytic solution and different numerical methods, such as split-step Crank–Nicolson [20] and Fourier spectral [21] methods, are used for its solution. We solve these equations numerically by the split-step Crank–Nicolson method using both real- and imaginary-time propagation. Imaginary-time simulation is employed to get the lowest-energy bound state of the boson–fermion quantum ball, while the real-time simulation is to be used to study the dynamics using the initial profile obtained in the imaginary-time propagation [22]. There are different C and FORTRAN programs for solving the GP equation [20, 22] and one should use the appropriate one. In the imaginary-time propagation the initial state was taken as in 6 and the width $w_i$ set equal to the variational widths. The convergence will be quick if the guess for the widths $w_i$ is close to the final converged width.

We consider the boson–fermion $^7\text{Li}$–$^6\text{Li}$ mixture in this study with the experimental scattering length $a_1 = a(^7\text{Li}) = -27.4a_0$. This negative scattering length imply intra-species attraction in $^7\text{Li}$. We also consider $a_1 = 100a_0$: it is also possible to have a boson–fermion quantum ball for for a repulsive boson–boson interaction and an attractive boson–fermion interaction. In the latter case the LHY correction is also effective. The fermions are considered to be in the weak-coupling BCS limit without any inter-species interaction between spin-up and -down fermions. The yet unknown inter-species scattering length $a_{12}$ is taken as a variable. The variation of $a_{12}$ and $a_1$ can be achieved experimentally by the optical [23] and magnetic [24] Feshbach resonance techniques.
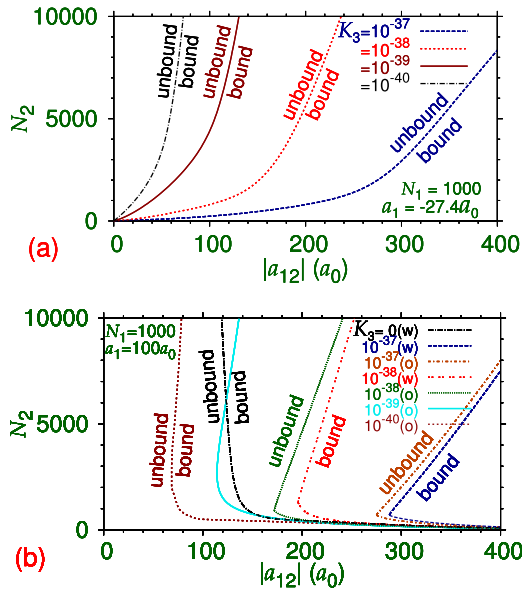
**Figure 1.** Variational $N_2 - a_{12}$ stability plot for the formation of boson–fermion $^7$Li–$^6$Li quantum ball of $N_1 = 1000$ bosons for $K_3 = 0, 10^{-37}$ m$^6$ s$^{-1}$, $10^{-38}$ m$^6$ s$^{-1}$, $10^{-39}$ m$^6$ s$^{-1}$, $10^{-40}$ m$^6$ s$^{-1}$, and for boson–boson scattering length (a) $a_1 = -27.4a_0$ and (b) $100a_0$. In (b) results are shown with (w) and without (o) the LHY correction term. The formation of the boson–fermion quantum ball is possible in the region to the right of each line marked 'bound'. No bound quantum ball is possible on the left side of the lines marked 'unbound'.

We consider the length scale $l_0 = 1$ $\mu$m and consequently, the time scale $t_0 = 0.11$ ms.

We find that a boson–fermion $^7$Li–$^6$Li quantum ball is achievable for a moderately attractive inter-species attraction (negative $a_{12}$) and for appropriate values of the number of atoms, for both attractive and repulsive boson–boson interaction. We illustrate in figure 1 the $N_2 - |a_{12}|$ variational stability plots for a boson–fermion quantum ball for boson–boson scattering lengths (a) $a = -27.4a_0$ and (b) $a = 100a_0$, for $N_1 = 1000$ and $K_3 = 0, 10^{-37}$ m$^6$ s$^{-1}$, $10^{-38}$ m$^6$ s$^{-1}$, $10^{-39}$ m$^6$ s$^{-1}$, and $10^{-40}$ m$^6$ s$^{-1}$. We find that a boson–fermion quantum ball can be formed for different non-zero values of $K_3$ with other parameters unchanged. However, a reduced $K_3$ value implies an increased net attraction, thus resulting in a more tightly bound boson–fermion quantum ball of reduced size. In the case of repulsive boson–boson interaction we also included the LHY correction. The stability plots are qualitatively different for attractive and repulsive boson–boson interaction. For an attractive boson–boson interaction a boson–fermion quantum ball can be formed for a weakly attractive boson–fermion interaction. However, for a repulsive boson–boson interaction a boson–fermion quantum ball can be formed for the boson–fermion attraction above a critical value.

In figure 2 we display similar variational and numerical $N_2 - |a_{12}|$ stability plots for $N_1 = 10\,000$ for (a) $a_1 = -27.4a_0$, (b) $a_1 = 100a_0$ (without LHY correction), and (c) $a_1 = 100a_0$ (with LHY correction) for different $K_3$ values. The numerical results for the stationary quantum balls in figures 2–5 are obtained by imaginary-time simulation. The formation of the boson–fermion quantum ball is possible on the right of the
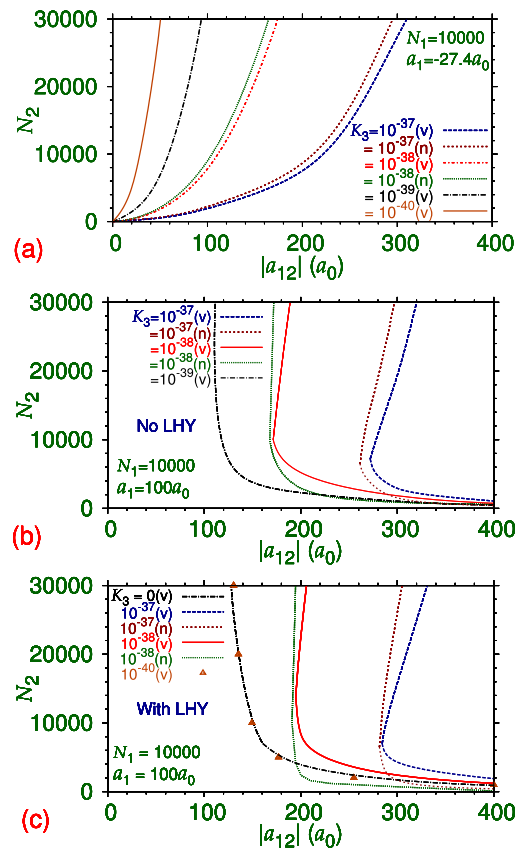


**Figure 2.** Variational (v) and numerical (n) $N_2 - a_{12}$ stability plot for the formation of boson–fermion $^7$Li–$^6$Li quantum ball of $N_1 = 10\,000$ bosons for different $K_3$ from 0 to $10^{-37}$ m$^6$ s$^{-1}$ and for boson–boson scattering length (a) $a_1 = -27.4a_0$, (b) $100a_0$ (without LHY correction), and (c) $100a_0$ (with LHY correction). The formation of boson–fermion quantum ball is possible only in the right side of these lines.

plotted lines in figures 1 and 2. There is not enough attraction on the left side of these lines to bind such a quantum ball. The numerical lines lie on the left of the variational lines showing a larger domain for the formation of the quantum balls. This is a consequence of the fact that the variational energies set an upper bound on the actual energy. Also the stability lines with the LHY correction correspond to an increased repulsion and the stability lines move towards right, viz. figures 2(b) and (c) implying a reduced domain in the parameter space for the formation of boson–fermion quantum ball.

From figures 1 and 2 we find that if the value of the parameter $K_3$ is suitably tuned, the effect of the three-body and LHY corrections on the formation of the binary ball could be quite similar. For example, compare the line $K_3 = 10^{-39}$ m$^6$ s$^{-1}$—without the LHY correction in figure 2(b)—with the line $K_3 = 0$—with LHY correction in figure 2(c)—and compare the same lines in figure 1(b). We also compared the corresponding shapes of the binary balls, which were also found to be similar. Hence, for a proper description of the binary boson-fermion balls, both the LHY and three-body corrections should be considered.

We used a Gaussian ansatz for the variational approximation, which is the eigenfunction of a harmonic oscillator. This ansatz should work well in the presence of a harmonic
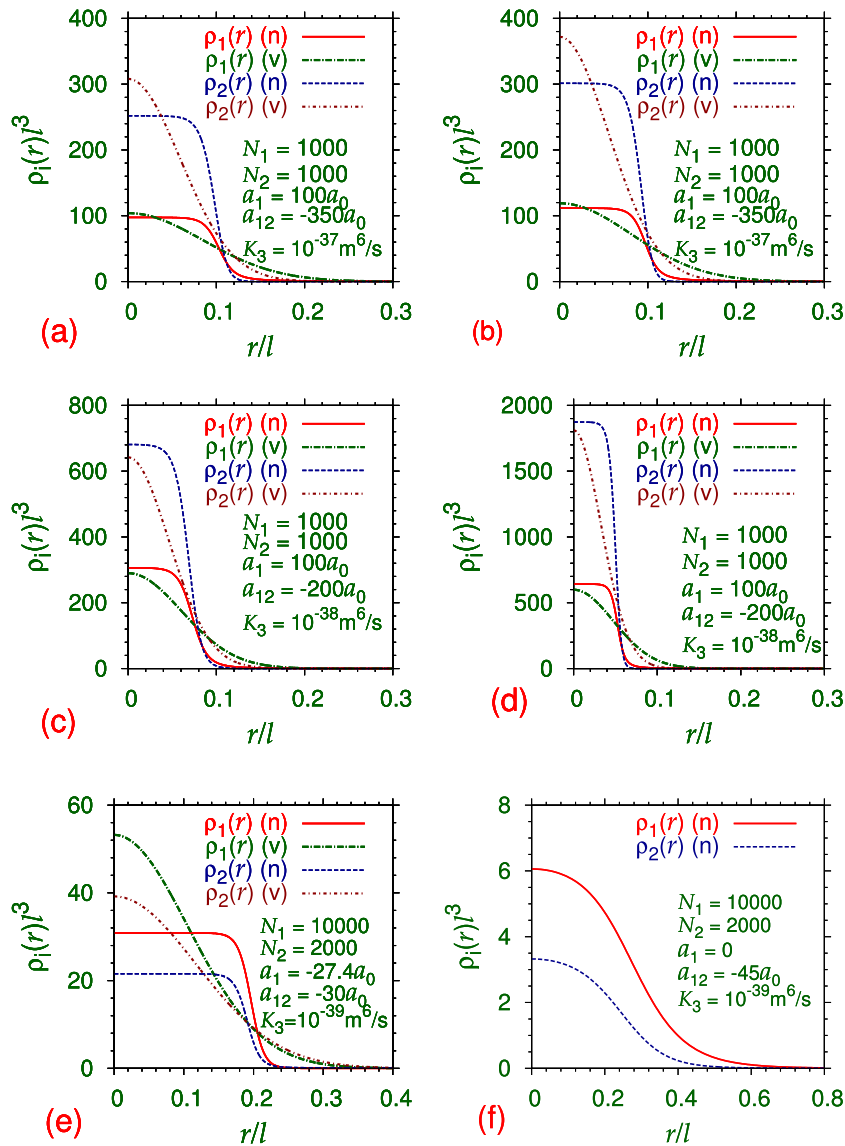
**Figure 3.** Variational (v) and numerical (n) densities $\rho_i = |\psi_i|^2$ of the bosons and fermions for different sets of parameters and for (a) $N_1 = N_2 = 1000, a_1 = 100a_0, a_{12} = -350a_0, K_3 = 10^{-37}$ m6 s$^{-1}$ with LHY correction, (b) $N_1 = N_2 = 1000, a_1 = 100a_0, a_{12} = -350a_0$, $K_3 = 10^{-37}$ m6 s$^{-1}$ without LHY correction, (c) $N_1 = N_2 = 1000, a_1 = 100a_0, a_{12} = -200a_0, K_3 = 10^{-38}$ m6 s$^{-1}$ with LHY correction, (d) $N_1 = N_2 = 1000, a_1 = 100a_0, a_{12} = -200a_0, K_3 = 10^{-38}$ m6 s$^{-1}$ without LHY correction, (e) $N_1 = 10\,000, N_2 = 2000, a_1 = -27.4a_0, a_{12} = -30a_0, K_3 = 10^{-39}$ m6 s$^{-1}$, (f) $N_1 = 10\,000, N_2 = 2000, a_1 = 0, a_{12} = -45a_0, K_3 = 10^{-39}$ m6 s$^{-1}$. The plotted quantities in this and following figures are dimensionless. The unit of length $l$ in all figures is $l = 1$ $\mu$m.

trap with small values of nonlinear interaction. In the present case, there is no harmonic trap and the nonlinearities could be quite large. Hence the variational approximation is not expected to be good in general. We have seen that the variational approximation has yielded qualitatively correct result for the stability plots, viz. figures 1 and 2. To test how well the variational approximation can yield the density profiles, we have compared in figure 3 the variational and numerical densities of the boson–fermion quantum ball for different cases for (a)–(b) $K_3 = 10^{-37}$ m$^6$ s$^{-1}$, (c)–(d) $10^{-38}$ m$^6$ s$^{-1}$, and (e)–(f) $10^{-39}$ m$^6$ s$^{-1}$. For repulsive boson–boson interaction, we have also included the LHY correction term in figures 3(a) and (c). The inclusion of LHY correction implies more repulsion: consequently, the density profiles are more extended in space with smaller central densities in these plots. In all cases the numerical densities are very different from a Gaussian shape.

Considering that there is no harmonic trap in the model, the agreement between the variational and numerical results is quite satisfactory.

Now we compare the variational and numerical energies of the boson–fermion quantum ball versus number of fermions in figure 4 for $N_1 = 10\,000$ and for (a) $a_1 = -27.4a_0, a_{12} = -70a_0, K = 10^{-39}$ m$^6$ s$^{-1}$ and (b) $a_1 = 100a_0, a_{12} = -350a_0, K = 10^{-37}$ m$^6$ s$^{-1}$. The variational energies are are always larger than the numerical energies. In figure 5 we plot the root-mean-square (rms) sizes $\langle r_1 \rangle$ and $\langle r_2 \rangle$ of bosons and fermions versus $N_2$ for $N_1 = 10\,000, a_1 = -27.4a_0$ and for (a) $a_{12} = -70a_0, K = 10^{-39}$ m$^6$ s$^{-1}$ and (b) $a_{12} = -150a_0, K = 10^{-38}$ m$^6$ s$^{-1}$. The agreement between the variational and numerical results is reasonable in both cases.

We have seen that these boson–fermion quantum balls are very tightly bound, viz. the large energy/boson in figure 4.
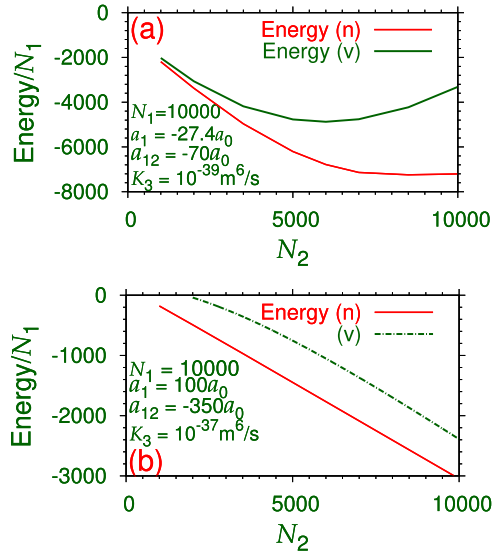
**Figure 4.** Variational (v) and numerical (n) energies versus $N_2$ for $N_1 = 10\,000$, and (a) $a_1 = -27.4a_0, a_{12} = -70a_0, K_3 = 10^{-39}$ m$^6$ s$^{-1}$ and (b) $a_1 = 100a_0, a_{12} = -350a_0, K_3 = 10^{-37}$ m$^6$ s$^{-1}$ without LHY correction. The unit of energy is $\hbar^2/(m_1 l^2)$.
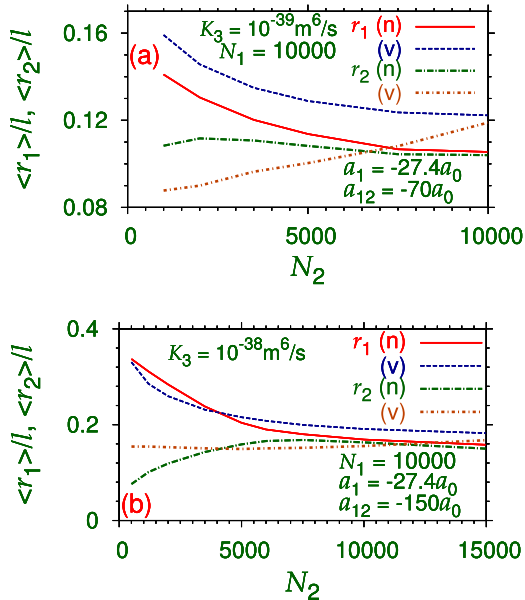


**Figure 5.** Variational (v) and numerical (n) rms sizes $\langle r_1 \rangle$ and $\langle r_2 \rangle$ versus $N_2$ for $N_1 = 10\,000$, $a_1 = -27.4a_0$ for (a) $K_3 = 10^{-39}$ m$^6$ s$^{-1}$, $a_{12} = -70a_0$ and (b) $K_3 = 10^{-38}$ m$^6$ s$^{-1}$, $a_{12} = -150a_0$.

The best way to observe these solitons is to prepare these boson–fermion quantum balls in a harmonic trap and then remove the trap. To this end we numerically prepared by imaginary-time propagation a boson–fermion quantum ball for $N_1 = 10\,000, N_2 = 2000, a_1 = 0, a_{12} = -45a_0, K_3 = 10^{-39}$ m$^6$ s$^{-1}$ in a harmonic trap of frequency $\omega = 2\pi \times 1443$ Hz which corresponds to a harmonic oscillator length $l \equiv \sqrt{\hbar/m_1\omega} = 1$ $\mu$m for $^7$Li atoms. Then we performed real-time propagation without a trap with the same parameters using the imaginary-time state as the initial state. In this simulation we have included an imaginary part to the three-body term $K_3$ to take into account the three-boson loss. There is
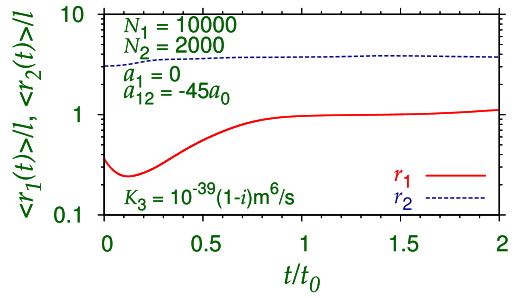


**Figure 6.** Dynamical oscillation of the rms sizes $\langle r_1, r_2 \rangle$ upon real-time propagation of the boson–fermion $^7$Li–$^6$Li quantum ball of figure 3(f) prepared by imaginary-time propagation in a harmonic trap of frequency $\omega = 2\pi \times 1443$ Hz. The plotted quantities are dimensionless. The harmonic oscillator length $l = 1$ $\mu$m, and the time scale $t_0 = 0.11$ ms.

estimate of three-body loss for $^7$Li atoms [25] for different values of scattering length $a_1$, although its value for $a_1 = 0$ is not given there. We take the three-body loss $K_3 = -i10^{-39}$ m$^6$ s$^{-1}$, which is the average value away from the nearby Feshbach resonance where $a_1 \to \pm\infty$. In the present real-time simulation we use $K_3 = (1-i)10^{-39}$ m$^6$ s$^{-1}$, which takes into account a realistic three-body loss. Due to the presence of the absorptive term in $K_3$, the number of bosons decay with time. Nevertheless, a smaller number of bosons is enough to keep the fermions bound due to the attractive boson–fermion inter-action. In figure 6 we plot the rms sizes of the bosons and fermions versus time. A practically constant rms size of the fermions guarantee the stability of the quantum ball. Due to a sudden introduction of the three-body loss term at $t = 0$ some disturbance is created in the quantum ball, as the initial state obtained by imaginary-time simulation is not an eigenstate of the absorptive Hamiltonian with three-body loss. The large values of the rms radius $r_2$ of fermions result due to some small noise at large values of $r$, although the quantum ball remain localized near the center.

## 4. Summary and discussion

We demonstrated the possibility of the creation of a stable, stationary, self-bound super-fluid boson–fermion quantum ball under attractive inter-species interaction using a variational and a numerical solution of a mean-field model. The boson–boson interaction could be attractive or repulsive. The collapse is avoided by a three-boson interaction and/or a LHY correction to the two-boson interaction. The static properties of the boson–fermion quantum ball are studied by the variational approximation and a numerical imaginary-time solution of the mean-field model. The dynamics is studied by a real-time solution of the same using the imaginary-time solution as input. The numerical and variational results for the rms radii, densities, and energies of the boson–fermion quantum ball are in agreement with each other.

The binary quantum ball is very tightly bound even for a small three-boson interaction and/or a small LHY correction, hence should be easy to observe in a laboratory like the boson–boson quantum ball [12]. We demonstrate a possible practical

mean for its formation. A boson–fermion mixture should be kept in a harmonic trap of harmonic oscillator length of few microns with parameters appropriate for the formation of a quantum ball. Actually, one of the easiest way of achieving a degenerate fermion gas is by sympathetic cooling in a boson–fermion mixture, such as in $^7$Li–$^6$Li [26]. Such a mixture should be used to create the boson–fermion quantum ball. Usually the size of the quantum ball will be much smaller than the harmonic oscillator length, indicating that the harmonic trap has no effect on the formation of the quantum ball. Consequently, the removal of the harmonic trap will have marginal effect on the quantum ball. To demonstrate this in numerical simulation, we form a quantum ball by imaginary-time propagation in a harmonic trap. Then we use the state so formed in a real-time propagation without a harmonic trap maintaining all other parameters the same. Bounded values of the rms radii in real-time propagation illustrates the stability of the quantum ball as well as the feasibility of its creation in a laboratory.

## Acknowledgments

## References

[1] Abdullaev F K, Gammal A, Kamchatnov A M and Tomio L 2005 *Int. J. Mod. Phys.* B **19** 3415
Kivshar Y S and Malomed B A 1989 *Rev. Mod. Phys.* **61** 763

[2] Kivshar Y S and Agrawal G 2003 *Optical Solitons: from Fibers to Photonic Crystals* (San Diego, CA: Academic)

[3] Strecker K E, Partridge G B, Truscott A G and Hulet R G 2002 *Nature* **417** 150
Khaykovich L, Schreck F, Ferrari G, Bourdel T, Cubizolles J, Carr L D, Castin Y and Salomon C 2002 *Science* **256** 1290
Cornish S L, Thompson S T and Wieman C E 2006 *Phys. Rev. Lett.* **96** 170401

[4] Petrov D S 2015 *Phys. Rev. Lett.* **115** 155302

[5] Lee T D, Huang K and Yang C N 1957 *Phys. Rev.* **106** 1135

[6] Adhikari S K 2005 *Phys. Lett.* A **346** 179
Pérez-García V M and Beitia J B 2005 *Phys. Rev.* A **72** 033620

[7] Adhikari S K 2017 *Phys. Rev.* A **95** 023606
Adhikari S K 2017 *Laser Phys. Lett.* **14** 025501

[8] Zhang Y-C, Zhou Z-W, Malomed B A and Pu H 2015 *Phys. Rev. Lett.* **115** 253902
Salasnich L and Malomed B A 2006 *Phys. Rev.* A **74** 053610
Salasnich L and Malomed B A 2013 *Phys. Rev.* A **87** 063625
Sakaguchi H, Li B and Malomed B A 2014 *Phys. Rev.* E **89** 032920
Gautam S and Adhikari S K 2018 *Phys. Rev.* A **97** 013629

Gautam S and Adhikari S K 2017 *Phys. Rev.* A **95** 013608
Gautam S and Adhikari S K 2015 *Laser Phys. Lett.* **12** 045501
Li Y, Luo Z, Liu Y, Chen Z, Huang C, Fu S, Tan H and Malomed B A 2017 *New J. Phys.* **19** 113043
Sakaguchi H and Malomed B A 2010 *Phys. Rev.* A **81** 013624

[9] Cappellaro A, Macri T, Bertacco G F and Salasnich L 2017 *Sci. Rep.* **7** 13358

[10] Kadau H, Schmitt M, Wenzel M, Wink C, Maier T, Ferrier-Barbut I and Pfau T 2016 *Nature* **530** 194
Ferrier-Barbut I, Kadau H, Schmitt M, Wenzel M and Pfau T 2016 *Phys. Rev. Lett.* **116** 215301
Chomaz L, Baier S, Petter D, Mark M J, Wächtler F, Santos L and Ferlaino F 2016 *Phys. Rev.* X **6** 041039

[11] Baillie D, Wilson R M, Bisset R N and Blakie P B 2016 *Phys. Rev.* A **94** 021602
Wächtler F and Santos L 2016 *Phys. Rev.* A **93** 061603
Xi Kui-Tian and Saito H 2016 *Phys. Rev.* A **93** 011604

[12] Cabrera C R, Tanzi L, Sanz J, Naylor B, Thomas P, Cheiney P and Tarruell L 2018 *Science* **359** 301
Cheiney P, Cabrera C R, Sanz J, Naylor B, Tanzi L and Tarruell L 2018 *Phys. Rev. Lett.* **120** 135301

[13] Semeghini G, Ferioli G, Masi L, Mazzinghi C, Wolswijk L, Minardi F, Modugno M, Modugno G, Inguscio M and Fattori M 2018 *Phys. Rev. Lett.* **120** 235301

[14] Adhikari S K 2005 *Phys. Rev.* A **72** 053608
Karpiuk T, Brewczyk K, Ospelkaus-Schwarzer S, Bongs K, Gajda M and Rzazewski K 2004 *Phys. Rev. Lett.* **93** 100401

[15] DeSalvo B J, Patel K, Johansen J and Chin C 2017 *Phys. Rev. Lett.* **119** 233401

[16] Adhikari S K and Salasnich L 2008 *Phys. Rev.* A **78** 043616

[17] Adhikari S K 2004 *Phys. Rev.* A **70** 043617

[18] Young-S L E and Adhikari S K 2012 *Phys. Rev.* A **86** 063611

[19] Pérez-Garcia V M, Michinel H, Cirac J I, Lewenstein M and Zoller P 1997 *Phys. Rev.* A **56** 1424
Muruganandam P and Adhikari S K 2012 *Laser Phys.* **22** 813

[20] Muruganandam P and Adhikari S K 2009 *Comput. Phys. Commun.* **180** 1888
Vudragovic D, Vidanovic I, Balaz A, Muruganandam P and Adhikari S K 2012 *Comput. Phys. Commun.* **183** 2021

[21] Adhikari S K and Muruganandam P 2003 *J. Phys. B: At. Mol. Opt. Phys.* **36** 2501

[22] Satarić B, Slavnić V, Belić A, Balaž A, Muruganandam P and Adhikari S K 2016 *Comput. Phys. Commun.* **200** 411
Lončar V, Balaž A, Bogojević A, Skrbić S, Muruganandam P and Adhikari S K 2016 *Comput. Phys. Commun.* **200** 406
Kishor Kumar R, Young-S L E, Vudragovic D, Balaz A, Muruganandam P and Adhikari S K 2015 *Comput. Phys. Commun.* **195** 117
Lončar V, Young-S L E, Škrbić S, Muruganandam P, Adhikari S K and Balaž A 2016 *Comput. Phys. Commun.* **209** 190
Young-S L E, Vudragović D, Muruganandam P, Adhikari S K and Balaž A 2016 *Comput. Phys. Commun.* **204** 209

[23] Enomoto K, Kasa K, Kitagawa M and Takahashi Y 2008 *Phys. Rev. Lett.* **101** 203201

[24] Inouye S, Andrews M R, Stenger J, Miesner H-J, Stamper-Kurn D M and Ketterle W 1998 *Nature* **392** 151

[25] Gross N, Shotan Z, Kokkelmans S and Khaykovich L 2009 *Phys. Rev. Lett.* **103** 163202

[26] Ferrier-Barbut I, Delehaye M, Laurent S, Grier A T, Pierce M, Rem B S, Chevy F and Salomon C 2014 *Science* **354** 1035